Inorganic Chemistry

Article

pubs.acs.org/IC

Structure, Phonon Properties, and Order−Disorder Transition in the Metal Formate Framework of $[NH_4][Mg(HCOO)_3]$

Mirosław Mączka,* Adam Pietraszko, Bogusław Macalik, and Krzysztof Hermanowicz

Institute of Low Temperature and Structure Research, Polish Academy of Sciences, P.O. Box 1410, 50-950 Wrocław 2, Poland

Supporting Information

ABSTRACT: We report the synthesis, crystal structure, thermal, dielectric, IR, and Raman studies of $[NH_4][Mg(HCOO)_3]$ formate. Single-crystal X-ray diffraction shows that it crystallizes in the hexagonal space group $P6_322$, with orientationally disordered NH_4^+ ions located in the cages of the network. Upon cooling, $[NH_4][Mg(HCOO)_3]$ undergoes a phase transition at around 255 K to the ferroelectric $P6_3$ structure. Raman and IR spectra show a strong increase in intensity of the N−H stretching bands as well as narrowing of the bands related to the NH_4^+ ions upon cooling. These changes indicate that the phase transition is due to orientational ordering of the NH_4^+ ions. Analysis of the Raman data show, however, that the rotational and translational motions of NH_4^+ do not freeze completely at the phase transition but exhibit further slowing down below 255 K, and the motional freezing becomes nearly complete below 140 K.

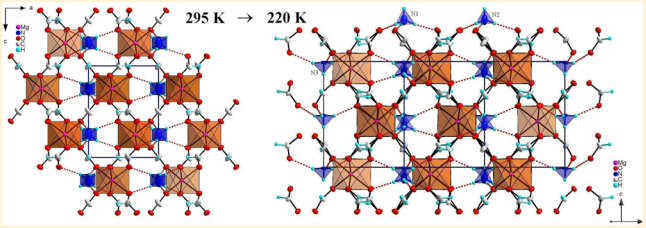

INTRODUCTION

Metal-organic frameworks (MOFs) have attracted a lot of attention in recent years due their wide spectrum of properties and possible applications. Among these, MOFs with two functionalities such as ferroelectricity and magnetism are particularly attractive candidates for use in electrically controllable microwave elements, magnetic-field sensors, and spintronics devices.[1] In this context, Wang et al. have reported a class of MOFs of formula $[(CH_3)_2NH_2][M(HCOO)_3]$ with M = Mn, Ni, Co, which show magnetic ordering at 8−36 K.[2] Later, Jain et al. reported electric ordering in $[(CH_3)_2NH_2][M(HCOO)_3]$ with M = Zn, Mn, Ni, Co, Fe at 160−185 K, thus showing that this class of materials can become multiferroic when the zinc is replaced by a transition metal ions.[3] It has been assumed that the electric ordering is antiferroelectric.[3] However, the observation of the good dielectric hysteresis loop for $[(CD_3)_2ND_2][Co(DCOO)_3]$ below T_c is very strong evidence that the low temperature structure of these materials is ferroelectric.[4] It is worth adding that nonmagnetic $[(CH_3)_2NH_2][Zn(HCOO)_3]$ has also been shown to exhibit a glassy behavior below T_c.[5] Very recently, a remarkable increase of a ferroelectric transition to ∼270 K was reported for $[(CH_3)_2NH_2][Mg(HCOO)_3]$.[6] Among other classes of metal formate frameworks templated by protonated amines, coexistence of magnetic and ferroelectric ordering was also reported at 8.0−29.3 and 191−254 K, respectively, for $[NH_4][M(HCOO)_3]$ with M = Mn, Fe, Ni, Co.[7] For nonmagnetic $[NH_4][Zn(HCOO)_3]$, Xu et al. reported a ferroelectric phase transition at 191 K.[8]

The metal formate frameworks templated by NH_4^+ or DMA^+ cation present a structure, in which the metal cations ($B = M^{2+}$) linked by the formate groups ($X = HCOO^-$) form the BX_3 skeleton, and the $A = DMA^+$ or NH_4^+ cations occupy the cavities.[6−8] The cations are disordered at room-temperature, and the onset of ferroelectricity at low temperatures has been associated with ordering of these cations.[5−8] The detailed mechanism of the ferroelectric phase transition in $[NH_4][M(HCOO)_3]$ is however still not well understood. It is even not clear if the phase transition is first- or second-order. We have, therefore, employed in the present studies vibrational spectroscopic techniques since they are very sensitive for long- and short-range ordering and structural changes. In particular, they are well suited to studies of hydrogen bonding and order−disorder phase transitions associated with motions of hydrogen atoms.

From an application point of view, it is important to find materials that exhibit ferroelectric properties at room temperature or as close as possible to room temperature. Literature data show that $[NH_4][Mn(HCOO)_3]$ exhibits ferroelectric properties already near 254 K.[7] A remarkable increase of a ferroelectric transition for $[(CH_3)_2NH_2][Mg(HCOO)_3]$, when compared to the Fe, Mn, Co, Zn, or Ni analogues, prompted us to look for a magnesium analogue of $[NH_4][M(HCOO)_3]$ in the hope that this compound would exhibit ferroelectricity already at room temperature. In this work, we report the synthesis and study of $[NH_4][Mg(HCOO)_3]$. This formate shows a phase transition at about 255 K, characterized by single crystal X-ray diffraction (XRD), differential scanning calorimetry (DSC), dielectric anomaly, and Raman and infrared (IR) spectroscopy.

Received: August 12, 2013
Published: January 3, 2014

   dx.doi.org/10.1021/ic4020702 | Inorg. Chem. 2014, 53, 787−794

EXPERIMENTAL SECTION

Synthesis. $MgCl_2$ (98%, Aldrich), $[NH_4][HCOO]$ (99%, Fluka), methanol (99.8%, Aldrich), and formic acid (98%, Fluka) were commercially available and used without further purification. Elemental analysis (C, H, N) was performed on a Elementar Vario EL CHNS analyzer. $[NH_4][Mg(HCOO)_3]$ was obtained by a slow diffusion method. This synthesis method is an adaptation of the previously reported one for the preparation of $[NH_4][Mn(HCOO)_3]$ compound.[8] In a typical experiment, a 16 mL methanol solution containing 12.8 mmol of $[NH_4][HCOO]$ and 12.8 mmol of formic acid was placed at the bottom of a glass tube (9 mm inner diameter). On this solution, a 16 mL methanol solution containing 1.6 mmol of $MgCl_2$ was gently added. The tube was sealed and kept undisturbed. Colorless, hexagonal plate crystals were harvested after 10 days. The yield is about 60% based on the starting magnesium salt. The product was washed by methanol and dried at 60 °C. Anal. Calcd: C, 20.31; H, 3.98; N, 7.90. Found: C, 20.40; H, 3.81; N, 7.82.

Crystallographic Structure Determination. Single-crystal data sets of the sample were collected at 295, 248, 220, and 120 K on a 4-circle diffractometer KM4CCD (Oxford Diffraction) using a graphite monochromated MoKα radiation (λ = 0.71073 Å). For the low temperature measurements, the crystal temperature was maintained using an open flow nitrogen cryosystem (Oxford Cryosystem). Thermal evolution of the lattice parameters was measured from 125 to 302 K with a step 10−15 K. Lattice parameters were obtained by a least-squares fit to 110 reflections. The CrysAlis software version 1.170.33.42 was used for data processing.[9] An empirical absorption correction was applied using spherical harmonics implemented in SCALE3 ABSPACK scaling algorithm. The structure was solved by direct methods and refined by the full-matrix least-squares method by means of SHELX-97 program package.[10] All measurements were carried out on the two samples.

In addition, powder XRD pattern was obtained on an X'Pert PRO diffractometer equipped with PIXcel ultrafast line detector, focusing mirror, and Soller slits for Cu Kα_1 radiation (λ = 1.54056 Å).

DSC. The DSC measurements of $[NH_4][Mg(HCOO)_3]$ were performed in the temperature range of 100−350 K on a DSC-7 instrument (Perkin-Elmer) at a rate of 15 °C/min under a nitrogen atmosphere with two cycles. Fresh crystalline powdered sample of 24.3 mg was used.

Dielectric Properties. The complex dielectric permittivity was measured at a frequency range from 10^0 to 10^6 Hz using a broadband impedance Alpha analyzer with Active Sample Cell (Novocontrol). The measurements were taken every 1 deg over the temperature range from 110 to 373 K. As the obtained single crystals were not big enough to perform single crystal dielectric measurements, a pellet made of well-dried sample was measured instead. The pellet with a diameter of 6 mm and thickness of 0.6 mm was located between gold electrodes with a diameter of 6 mm. The temperature values, with stability ±0.2 K, were changed by flow of vaporized liquid nitrogen heated and controlled by a self-made heating system.

Raman and IR Studies. Raman spectra were measured using a Bruker FT 100/S spectrometer with YAG:Nd laser excitation (1064 nm) and a helium-flow Oxford cryostat. Additional low-frequency Raman spectra were measured using a Renishaw InVia Raman spectrometer equipped with confocal DM 2500 Leica optical microscope, a thermoelectrically cooled CCD as a detector, and a diode laser operating at 830 nm. The sample was put in a Linkam cryostat cell THMS600. Temperature-dependent spectra were measured for the sample in Fluoroluble suspension in the range of 3800−400 cm^{-1} and in Apiezon N suspension in the range of 500−50 cm^{-1} using a helium-flow Oxford cryostat. The resolution was 2 cm^{-1} in all measurements.

RESULTS AND DISCUSSION

Thermal Properties. For the crystals harvested after 10 days of crystallization, the experimental powder XRD pattern matched well with the calculated one based on the single-crystal structure (Figure S1 in the Supporting Information), confirming the phase purity of the bulk sample. The DSC measurements show a heat anomaly at approximately 255 K (Figure 1). A λ-type anomaly suggests a second-order, reversible phase transition. The associated change in enthalpy ΔH and entropy ΔS was estimated to be ∼0.46 kJ mol^{-1} and ∼1.79 J mol^{-1} K^{-1}, respectively. The ΔH value is slightly larger than the ∼0.2−0.4 KJ mol^{-1} reported for other $[NH_4][M(HCOO)_3]$ compounds with M = Mn, Co, Fe, Ni, and Zn.[7] According to our X-ray diffraction studies, the NH_4^+ cation shows trigonal disorder in the high temperature (HT) phase (see discussion in the next paragraphs of the present paper). Knowing the change in entropy associated with the phase transition, it is possible to find the number of distinguishable positions of the cation in the low temperature (LT) phase from $\Delta S = R \ln(N2/N1)$, where N1 and N2 are the number of distinguishable positions of the NH_4^+ cation in the LT (ordered) and HT (disordered) phase, respectively. The entropy change found at the phase transition is ∼1.79 J mol^{-1} K^{-1}; that is, it is only about 31% of $R \ln 2$ = 5.8 J mol^{-1} K^{-1}, which is expected for a complete freezing of a two-way disordered system. This result indicates that the phase transition is more complex than expected on the basis of a simple order−disorder model.

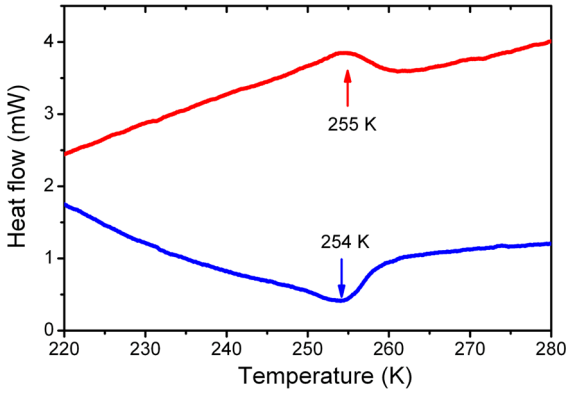

Figure 1. DSC traces for $[NH_4][Mg(HCOO)_3]$ in heating and cooling modes.

Dielectric Properties. The temperature dependence of the real component ε' of dielectric constant of powdered $[NH_4][Mg(HCOO)_3]$ is presented in Figure 2. This figure shows a broad dielectric anomaly that can be attributed to the

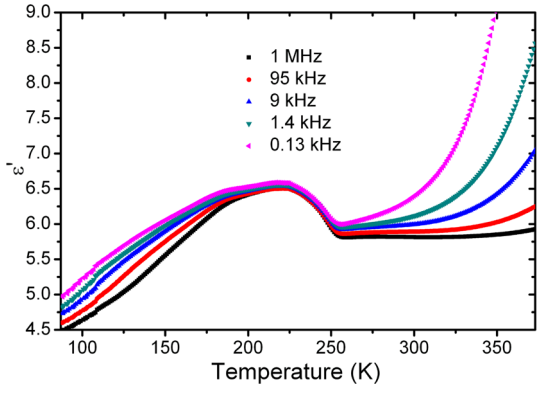

Figure 2. Temperature-dependent traces of the real part of the dielectric permittivity, ε', for powdered $[NH_4][Mg(HCOO)_3]$ at 0.13, 1.4, 9, 95, and 1000 kHz.

dx.doi.org/10.1021/ic4020702 | Inorg. Chem. 2014, 53, 787−794

onset of the phase transition, in agreement with the DSC results. The main peak position displays slight frequency dependence. Similar broad dielectric anomaly was reported for powdered $[NH_4][Zn(HCOO)_3]$ at about 180 K.[11] It is worth mentioning that the temperature dependence of ε' under an applied electric field $E \parallel c$ of the single-crystal $[NH_4][Zn(HCOO)_3]$ showed a narrower dielectric anomaly at T_c = 191 K with a much larger ε' value at the peak position when compared to the powdered $[NH_4][Zn(HCOO)_3]$.[8,11] This anomaly was attributed to onset of a ferroelectric ordering in the low temperature phase, and ferroelectricity of $[NH_4][Zn(HCOO)_3]$ was confirmed by the presence of a very clear dielectric hysteresis loop.[11] Pronounced similarity between dielectric anomalies observed here for $[NH_4][Mg(HCOO)_3]$ and reported for $[NH_4][Zn(HCOO)_3]$ indicates that they have the same origin; that is, they can be attributed to onset of a ferroelectric ordering in the low temperature phase. Our results also show that the dielectric constant, measured at low frequency, increases rapidly above 300 K with temperature. This temperature dependence can be most likely attributed to an increase in conductivity of $[NH_4][Mg(HCOO)_3]$ above 300 K due to the presence of some slight amount of water in the studied sample. The temperature evolution of the imaginary component ε'' of the dielectric constant of powdered $[NH_4][Mg(HCOO)_3]$ is also in agreement with contribution of the conductivity in this material above 300 K (see Figure S2, Supporting Information).

Structural Studies. The single-crystal X-ray diffraction studies performed in the 120−295 K range show that $[NH_4][Mg(HCOO)_3]$ belongs to two hexagonal polymorphic structures. At 295 K, the compound crystallizes in the $P6_322$ space group (with small unit cell of 377.78 Å^3), while it undergoes a phase transition into the $P6_3$ structure at T_c = 255 K (with a large unit cell of 1124.3 Å^3). The details of data collection, data reduction, and crystallographic data are summarized in Tables S1−S4, Supporting Information. In the following paragraphs, we will describe the main characteristics of these structures.

The temperature dependence of lattice parameters has not yet been reported for $[NH_4][M(HCOO)_3]$ compounds with M = Mn, Co, Fe, Ni, and Zn, but our XRD data show that in the HT phase of $[NH_4][Mg(HCOO)_3]$ both parameters a and c decrease upon cooling (see Figure 3). It is interesting to notice that this behavior is different from that observed under pressure for $[NH_4][Zn(HCOO)_3]$, which exhibited negative compressibility in the c direction.[12]

Room Temperature Structure. $[NH_4][Zn(HCOO)_3]$ is isostructural to other $[NH_4][M(HCOO)_3]$ compounds with M = Mn, Co, Fe, Ni, and Zn.[7,8] Each magnesium cation is connected to its six magnesium nearest neighbors through six formate bridges in an octahedral environment where the Mg−O distance is 2.0907 Å (see Figures 4 and S3, Supporting Information). The NH_4^+ cations are located in hexagonal channels along the c axis. These cations show trigonal disorder and N−H···O hydrogen bonds to the anionic framework (Table S4, Supporting Information). It is worth pointing out that the c/a ratio of the lattice parameters of 1.153, 1.135, 1.121, 1.118, and 1.101 for the Mn, Fe, Co, Zn, and Ni compounds, respectively,[7,8] exhibits a systematic decrease with the decrease in the ionic radii in the sequence Mn^{2+} (0.97 Å), Fe^{2+} (0.92 Å), Co^{2+} (0.89 Å), Zn^{2+} (0.88 Å), and Ni^{2+} (0.83 Å).[13] $[NH_4][Mg(HCOO)_3]$ behaves however in a different way; that is, the c/a ratio for this compound is anomalously large (1.129), in spite of its small ionic radius of 0.86 Å. This effect can be most likely rationalized by formation of stronger H-bonds between NH_4^+ and anionic framework.

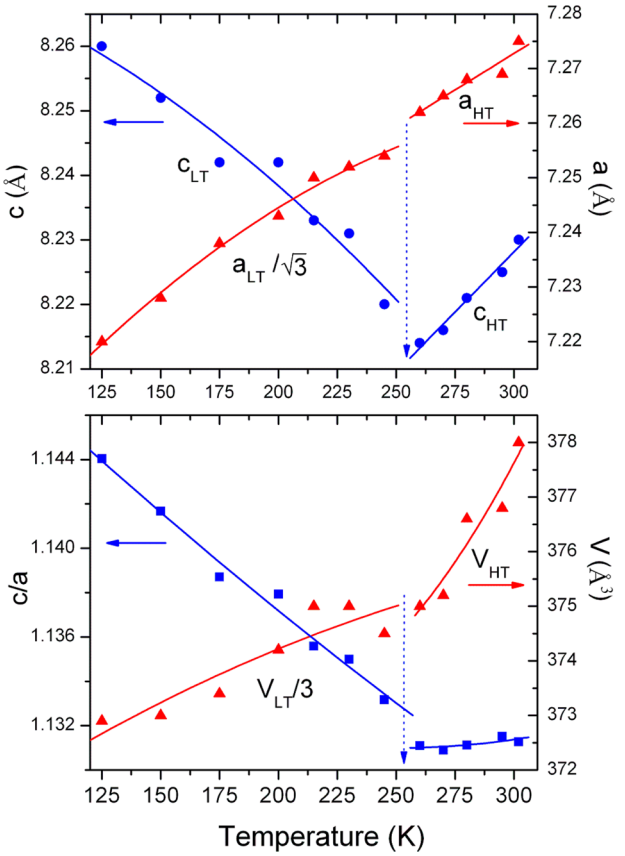

Figure 3. Evolution of the a and c axes, unit cell volume, and c/a ratio as a function of temperature for the LT and HT phases. Experimental data are shown as squares and circles. Solid lines are shown to guide the eye.

Crystallographic Structures at 248, 220, and 120 K. The temperature dependence of the lattice parameters and unit cell volume shows a very clearly onset of the phase transition at about 255 K (see Figure 3). Character of these changes suggests that the phase transition is second-order. Interestingly, $[NH_4][Mg(HCOO)_3]$ exhibits below T_c negative thermal expansion along the c axis.

The structure of $[NH_4][Mg(HCOO)_3]$ shows hexagonal symmetry ($P6_3$ space group) below T_c. This result shows that $[NH_4][Mg(HCOO)_3]$ undergoes the same structural changes during the phase transition as described previously for other $[NH_4][M(HCOO)_3]$ compounds with M = Mn, Fe, Ni, Co, Zn.[7,8] In brief, the phase transition is associated with ordering of the NH_4^+ cations. Each of the three unique NH_4^+ cations in the LT phase has one apical and three basal N−H bonds. Moreover, NH_4^+ cations shift along the c direction by the d values in the ranges 0.391−0.485 Å (at 120 K, see Table S4, Supporting Information), with respect to the anionic framework. As discussed by Xu et al.,[7] these shifts in the LT phases directly result in the appearance of spontaneous polarization (P_S) in these MOFs. The P_S values for $[NH_4][Mg(HCOO)_3]$ estimated in the same way as proposed by Xu et al. are about 0.02, 0.58, and 0.93 μC cm^{-2} at 248, 220, and 120 K, respectively (see Table S4). These data show that the estimated P_S value for $[NH_4][Mg(HCOO)_3]$ at 120 K is comparable to

dx.doi.org/10.1021/ic4020702 | Inorg. Chem. 2014, 53, 787−794

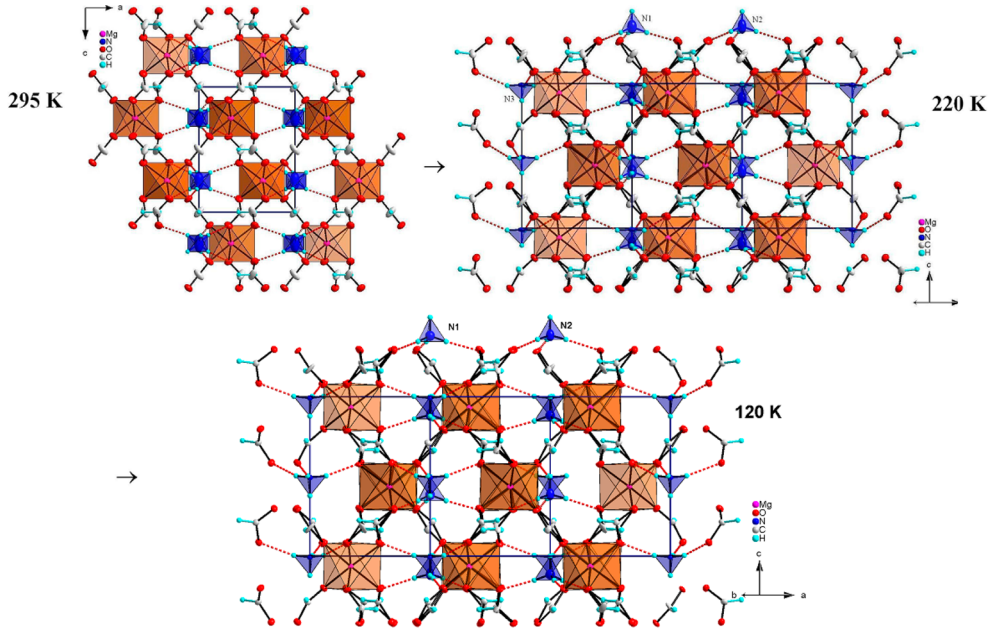

Figure 4. Structure of $[NH_4][Mg(HCOO)_3]$ at 295, 220, and 120 K, viewed along the direction perpendicular to the *c* axis. Thermal ellipsoids for N atoms of NH_4^+ are shown in blue and strong H-bonds are shown by dotted red lines.

the P_S value of 0.94−1.03 μC cm^{-2} estimated for other $[NH_4][M(HCOO)_3]$ compounds with M = Mn, Fe, Ni, Co, Zn at 110 K.[7] Our data also show that the estimated P_S value is very small near T_c but increases significantly with decreasing temperature, as expected for a second-order phase transition.

In the LT phase, each basal N−H bond forms a strong H-bond to the metal formate framework, with N···O distance of 2.8369−2.8737 Å and N−H···O angle of 163.0−176.1° (at 120 K, see Table S4). In addition, the basal N−H bond of NH_4^+ shifted in the (+*c*) direction forms an additional weak H-bond, with N···O distance of 3.1031 Å and N−H···O angle of 113.8° (at 120 K). Xu et al. suggested that in other $[NH_4][M(HCOO)_3]$ compounds with M = Mn, Fe, Ni, Co, Zn, the apical N−H bond, with the N−H directing along the *c* axis, forms a trifurcated weak hydrogen bond, with N···O distances of 3.075−3.152 Å and N−H···O angle of 103−110°.[7] Our XRD data obtained at 120 K for $[NH_4][Mg(HCOO)_3]$ show that for the apical N−H bond, the N···O distances are 3.075−3.143 Å and N−H···O angles are 102.8−104.0° (see Table S4). These values are comparable to those reported by Xu et al. for other $[NH_4][M(HCOO)_3]$ compounds.[7] However, it should be noticed that the H···O distances are very large (2.730−2.779 Å), and the N−H···O angles are far from linear. Therefore, these contacts can be regarded as extremely weak H-bonds. XRD data show also that the N···O distances decrease significantly with decreasing temperature for NH_4^+ shifted in the (−*c*) direction (see Table S4), implying an increase of the H-bond strength. In contrast to this behavior, for NH_4^+ shifted in the (+*c*) direction very weak changes in the N···O distances, and thus the strength of the H-bond can be observed upon cooling.

Our XRD data reveal also another interesting feature of $[NH_4][Mg(HCOO)_3]$. In the HT phase, N atoms of NH_4^+ show large principal mean square atomic displacements in the *c* direction, indicating significant mobility of the NH_4^+ ions in this direction (calculation of the crystal structure for the positional model assuming two N atoms showed the split of about 0.45 Å along the *c* direction). In the LT phase, NH_4^+ shift with respect to the metal formate framework and at 120 K all N atoms show normal thermal ellipsoids (see Table S3 and Figure S3). Very similar behavior also was observed for other $[NH_4][M(HCOO)_3]$ compounds with M = Mn, Fe, Ni, Co, Zn, and it was concluded that the potential well for NH_4^+ movement changes from a quite flat single well at HT to a double well at LT.[7] Our results for $[NH_4][Mg(HCOO)_3]$ are consistent with this conclusion, but they also show that near T_c, principal mean square atomic displacements of N atoms are different for NH_4^+ shifted in the (−*c*) and (+*c*) directions. Just below T_c, i.e., at 248 K, N3 atoms of NH_4^+ shifted in the (+*c*) direction exhibit a small principal mean square atomic displacements in all directions, indicating weak mobility in the *c* direction in the LT phase even close to T_c (see Table S3). In contrast to this behavior, N1 and N2 atoms of NH_4^+ shifted in the (−*c*) direction exhibit large principal mean square atomic displacements along the *c* direction at 248 K. These displacements decrease upon cooling, and at 120 K the N1 and N2 atoms show normal thermal ellipsoids. This result indicates that translational dynamics of these NH_4^+ cations is still important in the LT phase, but it becomes less pronounced upon cooling. It should be noted that there is a clear correlation between H-bond strength and value of principal mean square atomic displacements along the *c* direction. This result proves that H-bonds play a major role in slowing of the correlated rotational and translational motions of the NH_4^+ ions and the mechanism of the phase transition.

Vibrational Studies. The vibrational spectra of $[NH_4][Mg(HCOO)_3]$ may be understood by dividing **k** = 0 vibrations into internal vibrations of the ammonium and formate ions, and the lattice vibrations. The fundamental internal vibrations of the free NH_4^+ cation consist of the totally symmetric nondegenerate stretching mode ν_1, the triply degenerate antisymmetric stretching mode ν_3, the doubly degenerate symmetric bending mode ν_2, and the triply degenerate antisymmetric bending mode ν_4.[14] The lattice modes of NH_4^+ cation consist of the triply degenerate translational mode ν_5 and librational mode $\nu_6(F_1)$.[14] The

dx.doi.org/10.1021/ic4020702 | *Inorg. Chem.* 2014, 53, 787−794

fundamental internal vibrations of the free $HCOO^-$ ion consist of the C−H stretching mode ν_1, the symmetric C−O stretching mode ν_2, the antisymmetric C−O stretching mode ν_4, the symmetric O−C−O bending (scissor) mode ν_3, the C−H in-plane bending mode ν_5, and the C−H out-of-plane bending mode ν_6.[15] There are also translational modes related to the Mg^{2+} cations and $HCOO^-$ anions as well as librational modes of the $HCOO^-$ anions.

The Raman and IR spectra of $[NH_4][Mg(HCOO)_3]$ are presented in Figures 5, 6, and S4−S7, and the observed IR and Raman frequencies (in cm^{-1}) are listed in Table 1 together with suggested assignments that were mostly based on literature data.[7,14,15] The bands observed in the range of 3800−800 cm^{-1} are characteristic for internal modes of the NH_4^+ ion and the $HCOO^-$ group (Table 1). The suggested assignments in Table 1 agree well with that proposed for $[NH_4][M(HCOO)_3]$ with M = Mn, Co and Ni.[7] It is worth pointing out however that we propose different assignments for a few bands. First, Wang et al. assigned the IR band at 2929−2938 cm^{-1} to the $2\nu_4$ mode.[7] Our results show that the corresponding band of $[NH_4][Mg$

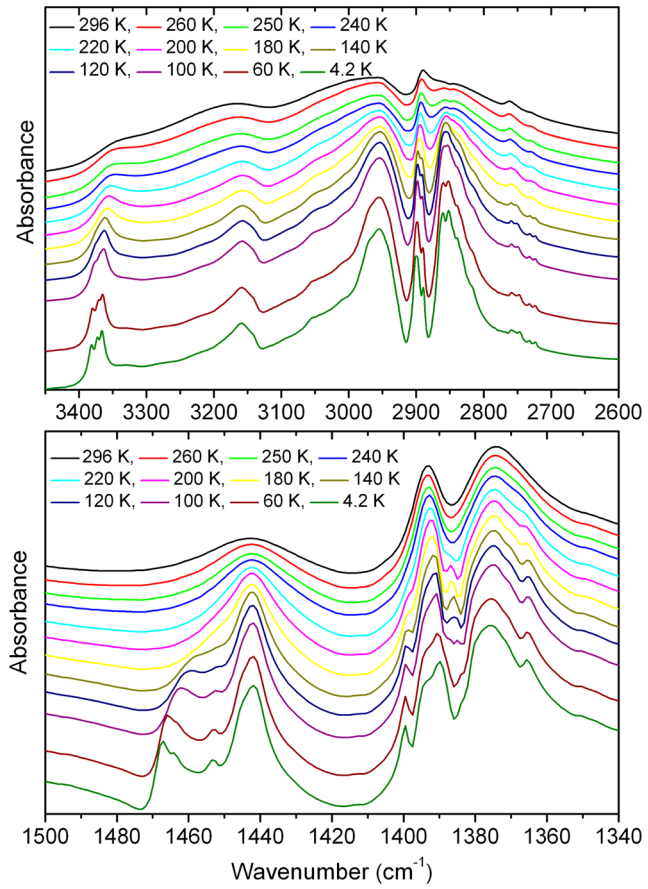

Figure 5. Detail of the IR spectra results corresponding to the spectral ranges 2600−3450 and 1340−1500 cm^{-1}.

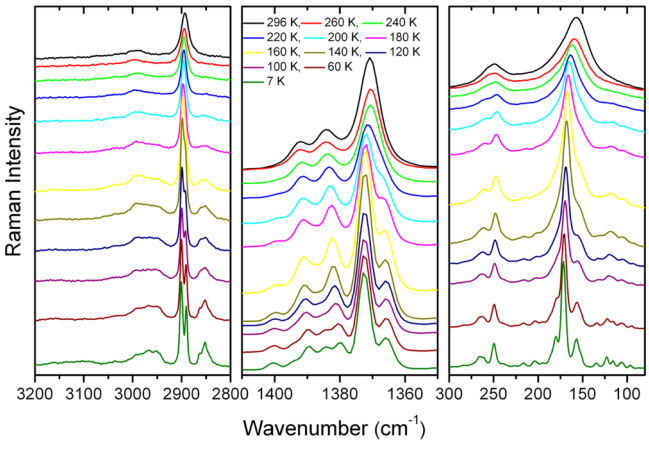

Figure 6. Detail of the Raman spectra results corresponding to the spectral ranges 2800−3200, 1320−1450 and 80−300 cm^{-1}.

Table 1. IR and Raman Frequencies (in cm^{-1}) of $[NH_4][Mg(HCOO)_3]$ and Suggested Assignments[a]

IR 300 K	IR 5 K	Raman 300 K	Raman 5 K	assignment
3337sh	3382m, 3372m, 3366m, 3326w		3381vw, 3372vw, 3367vw	$\nu_3(NH_4^+)$
3165m	3273w, 3219w, 3158m, 3145sh		3159w, 3136w, 3092w	$\nu_3(NH_4^+)$
3042sh	3053w, 3044w		3035vw	$\nu_1(NH_4^+)$
2990sh	3005sh	2992w	2990w	$\nu_4(HCOO^-)$ + $\nu_5(HCOO^-)$
2953m	2968sh, 2955m		2967w, 2953w	$\nu_3(NH_4^+)$
2890m	2900m, 2898m, 2890w	2893m	2901m, 2890m	$\nu_1(HCOO^-)$
2860w	2861m, 2852m		2862w, 2852w	$\nu_3(NH_4^+)$
2842m	2838m, 2833sh, 2816sh		2839sh	$\nu_3(NH_4^+)$
2761w	2759w, 2747w	2763w	2746vw	$2\nu_5(HCOO^-)$
2729sh	2732w, 2724w			$2\nu_2(HCOO^-)$
		2147w	2149w, 2141w	$\nu_2(HCOO^-)$ + $\nu_3(HCOO^-)$
1691sh		1686w	1711w, 1689w	$\nu_2(NH_4^+)$
1597s	1600s, 1593s, 1562w	1593w	1593w, 1562w, 1535w	$\nu_4(HCOO^-)$
1441m	1467m, 1464w, 1453w, 1442m	1434w	1466w, 1453w, 1444w, 1429vw, 1417vw	$\nu_4(NH_4^+)$
1393s	1399w, 1394sh, 1390s	1392m	1400w, 1394sh, 1389m	$\nu_5(HCOO^-)$
		1384m	1380m, 1384m	$\nu_5(HCOO^-)$
1374s	1375s, 1366w	1371s	1372s, 1365m	$\nu_2(HCOO^-)$
		1348w	1350w	overtone or combination
		1078w	1082w, 1075w	$\nu_6(HCOO^-)$
808m	813m	812sh, 804m	817w, 811sh, 806m	$\nu_3(HCOO^-)$
			408vw	$T'(Mg^{2+})$
377sh, 358s	387s, 359s, 330w	343w	353w, 331vw, 319vw	$T'(Mg^{2+})$ and $L(NH_4^+)$
276w	293w, 284m, 264w	256sh	283w, 265m, 262m	$T'(NH_4^+)$
		249m	249m, 240w	$T'(HCOO^-)$
223m	229s, 215w		225vw, 216w, 203w, 194w	$T'(HCOO^-)$
179m	203m, 188m, 171m			$T'(HCOO^-)$
		157s	180m, 171s, 157m, 152sh	$L(HCOO^-)$
114w	130m		135w, 123w, 115w, 106w, 96w	$L(HCOO^-)$
		72sh	**73m**	$L(HCOO^-)$
		57s	**58m**	$L(HCOO^-)$

[a]Key: s, strong; m, medium; w, weak; vw, very weak; sh, shoulder. Values in bold correspond to the additional low-frequency Raman data obtained at 296 and 82 K.

dx.doi.org/10.1021/ic4020702 | Inorg. Chem. 2014, 53, 787−794

$(HCOO)_3]$, observed at 2953 cm^{-1}, is very broad, and its intensity increases with decreasing temperature (Figures 5 and S4, Supporting Information). The Raman spectrum does not show any clear band near 2950 cm^{-1}, but clear bands become visible at low temperatures (see Figures 6 and S6, Supporting Information). This behavior proves that this band is not an overtone of the ν_4 mode but should be assigned to stretch of the N−H bonds. Second, Wang et al. assigned the band at 3330−3335 cm^{-1} to a combination mode of the NH_4^+ ion: $\nu_1 + \nu_5$.[7] Our results show that the corresponding IR band of $[NH_4][Mg(HCOO)_3]$, observed at 3337 cm^{-1}, splits at low temperatures into four narrow bands. This behavior suggests that the 3337 cm^{-1} band also involves vibrations of the N−H bonds. Indeed, literature data show that similar narrow bands are usually observed near 3300 cm^{-1} for the ammonium salts with weak H-bonds.[16]

The bands observed below 400 cm^{-1} can be attributed to lattice modes. The translational modes of the ammonium groups are expected in the frequency region of 170−270 cm^{-1}, and the librational modes in the 300−380 cm^{-1} region.[14,17] The translational and librational modes of the formate groups were typically observed below 250 cm^{-1},[18] and translational mode of the Mg^{2+} cations in the 330−380 cm^{-1} region.[19] We assign tentatively the bands below 250 cm^{-1} to the librational and translational modes of the formate groups, the bands in the frequency region of 310−390 cm^{-1} to the translational modes of the Mg^{2+} cations and librational modes of the formate groups, and the bands in the 260−300 cm^{-1} region to the translational modes of the ammonium groups.

Former study of $[NH_4][M(HCOO)_3]$ compounds with M = Mn, Co and Ni showed that the frequencies of the symmetric and antisymmetric carboxylate modes of the formate ion are not affected by the changes of the framework for different M^{2+} cations.[7] The corresponding IR active modes of $[NH_4][Mg(HCOO)_3]$ show however a significant shift to higher frequencies. For instance, the antisymmetric stretching mode shifts from 1575 to 1583 cm^{-1} for $[NH_4][M(HCOO)_3]$ compounds with M = Mn, Co, and Ni,[7] to 1597 cm^{-1} for $[NH_4][Mg(HCOO)_3]$, reflecting a larger strength of the C−O bonds in the magnesium compound.

Our IR study also shows that the frequency of the C−H stretching mode of the formate ion is observed at 2890 cm^{-1} (Table 1). The corresponding IR modes of the Mn, Co, and Ni analogues were observed at 2870, 2887, and 2894 cm^{-1}, respectively.[7] This comparison shows that frequency of this mode increases with the decrease in the ionic radii.

Temperature-Dependent Raman and IR Study, and Mechanisms of the Phase Transition. Temperature-dependent Raman and IR studies show a pronounced increase of the full width at half-maximum (fwhm) upon heating for the bands assigned to stretching and bending vibrations of NH_4^+, whereas the bands related to internal modes of $HCOO^-$ exhibit relatively weak changes (Figures 5−7, S4 and S6). This behavior proves that the phase transition in $[NH_4][Mg(HCOO)_3]$ has an order−disorder character and is governed by dynamics of the NH_4^+ cations. Interestingly, a very pronounced increase in fwhm upon heating is also observed for the lattice modes, including translational and librational modes of $HCOO^-$ (Figures 6, S6 and S7). Different temperature dependence of fwhm for the internal and lattice modes of $HCOO^-$ reflects different sensitivity of these modes to short- and long-range order; that is, external modes are very sensitive to long-range order, whereas the internal modes depend mainly on short-range order. When the temperature decreases, Raman and IR bands shift toward lower or higher frequency, and many of them split into a few components. Some of the bands also exhibit significant increase of intensity. It can be also noticed that many new bands appear at low temperatures, especially in the low frequency region below 400 cm^{-1}. The observed changes indicate lowering of crystal symmetry.

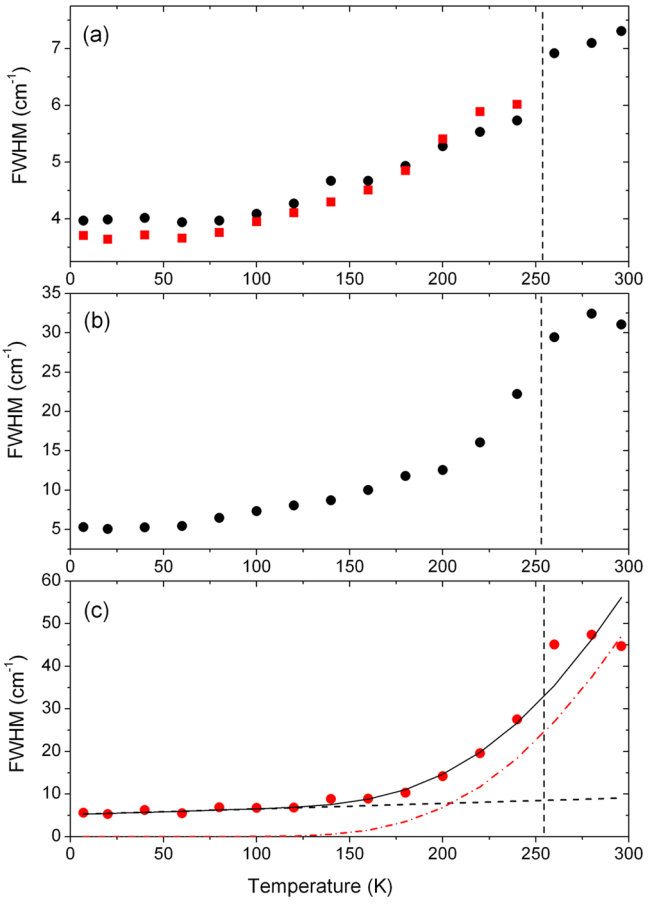

Figure 7. Temperature dependence of fwhm of (a) the 1372 cm^{-1} (circles) and 1365 cm^{-1} (squares) Raman bands corresponding to the $\nu_2(HCOO^-)$ mode, (b) the 250 cm^{-1} band corresponding to the $T'(HCOO^-)$ mode, and (c) the 1444 cm^{-1} band corresponding to the $\nu_4(NH_4^+)$ mode. The vertical lines indicate the temperature at which $[NH_4][Mg(HCOO)_3]$ undergoes the phase transition. The solid line in (c) is fit on the data to eq 1. The black dash line and red dash dot lines represent contribution due to anharmonicity and reorientational processes, respectively.

The NH_4^+ cation is orientationally disordered at room temperature and forms N−H···O hydrogen bonds to the metal-formate framework, with a N···O distance of 2.9905 Å. In the low temperature structure, each basal (apical) N−H bond forms a strong (weak) H-bond to the metal formate framework, with a N···O distance of 2.8369−2.8737 Å (3.075−3.143 Å) (at 120 K). It is well-known that the strength of the individual N−H···O hydrogen bond can be estimated by correlating the individual N···O distance with N−H stretching frequency.[20,21] Very weak N−H···O hydrogen bonds in ammonium salts give an N−H stretching frequency and $\nu_4(NH_4^+)$ bending mode frequency typically around 3300 and 1400 cm^{-1}, respectively.[21] With increasing strength of the N−H···O hydrogen bond, the N−H stretching modes shift to lower frequencies whereas the

dx.doi.org/10.1021/ic4020702 | Inorg. Chem. 2014, 53, 787−794

$\nu_4(NH_4^+)$ mode shifts to higher energies. For instance, a former study of NH_4VO_3 showed that the three N−H stretching bands at around 2800, 2950, and 3190 cm^{-1} could be assigned to the N−H···O hydrogen bonds with the N···O distance (N−H···O bond angle) of 2.792 Å (171°), 2.846 Å (179°), and 2.992 Å (123°).[21] Our Raman and IR spectra show that the N−H stretching modes (bending $\nu_4(NH_4^+)$ modes) are observed in a broad frequency range of 2816−3382 cm^{-1} (1417−1467 cm^{-1}) (at 5 K). This result points to large distribution of the N−H bond lengths and N−H···O bond angles in the crystal structure. As mentioned above, the hydrogen bond of the apical N−H group is very weak: the N···O distances of 3.075−3.143 Å (at 120 K) are longer than the longest N···O distance of 2.992 Å observed in NH_4VO_3. We can expect, therefore, that the corresponding N−H stretching mode will be observed at higher frequency than the 3190 cm^{-1} mode of NH_4VO_3. We can therefore assign the bands in the 3326−3382 cm^{-1} to the N−H stretching modes of the N−H apical groups. Small width of these bands and their shift to lower frequency upon heating are consistent with this assignment. The basal N−H group forms much stronger hydrogen bond, similar to the stronger hydrogen bonds found in NH_4VO_3, for which the N···O distances were 2.792 and 2.846 Å.[21] We may expect that the corresponding N−H stretching modes will also be observed at similar frequencies as in NH_4VO_3, i.e., close to 2800−2950 cm^{-1}. This assumption is consistent with our data that show the presence of bands in the 2816−2862 and 2953−2968 cm^{-1}, which exhibit pronounced narrowing at low temperatures. Our Raman spectra also show that the N−H stretching modes have negligible intensity at room temperature, but they become very clearly observed at low temperatures. Strong decrease in intensity of these modes at high temperatures reflects highly dynamic nature of hydrogen bonds.

Low-frequency Raman spectra also show pronounced narrowing of the 57 and 72 cm^{-1} bands upon cooling (see Figure S6). These spectra do not show any softening of the low frequency modes observed above 20 cm^{-1}, in agreement with an order−disorder character of the phase transition in $[NH_4][Mg(HCOO)_3]$. However, we cannot exclude a possibility that there is a soft mode below the frequency range of the measurements.

It is well-known that the band broadening in molecular crystals is mainly due to anharmonism and reorientation of molecules or ions. When dynamic disorder prevails over the phonon decay process, the width of band is usually defined as

$$\text{fwhm} = A + BT + C\exp(-E_a/kT) \quad (1)$$

where E_a is the activation energy, k is the Boltzmann constant, and T is the temperature.[22] The constant A accounts for the broadening arising from factors other than the phonon decay, such as structural and compositional defects. The second and third term of eq 1 represents the influence of anharmonicity and thermally activated reorientational processes, respectively. Equation 1 enables us to determine the activation energy of reorientational processes for NH_4^+ in $[NH_4][Mg(HCOO)_3]$ using temperature dependence of the fwhm for the $\nu_4(NH_4^+)$ Raman active mode observed at 1444 cm^{-1} (Figure 7). The fit on the data to eq 1 gives A = 5.2 cm^{-1}, B = 0.013 cm^{-1} K^{-1}, C = 2638.8 cm^{-1}, and E_a = 103 meV (9.94 KJ/mol or 1195 K). The value of E_a is about twice as large as the 54 meV (5.21 KJ/mol or 627 K) value found for $K_{0.18}(NH_4)_{0.82}H_2PO_4$ crystal[22] but significantly smaller than the 560 meV (54.0 KJ/mol or 6500 K) found for $(NH_4)_2Cr(O_2)_4$.[17] It should be noted that our analysis indicate that the contribution of the reorientational processes to the observed broadening become important above 140 K, whereas below 140 K the observed changes in fwhm are mainly related to the anharmonic contribution.

To obtain deeper insight into mechanism of the phase transition, we have also analyzed temperature dependence of splitting for three Raman bands observed at 2893, 1371, and 1078 cm^{-1} at room temperature. Figure S8, Supporting Information shows that splitting of these bands increases continuously below T_c, without any clear jump at T_c. This behavior indicates that the phase transition is a second-order one.

As mentioned above, a remarkable increase of a ferroelectric transition to ∼270 K was reported for $[(CH_3)_2NH_2][Mg(HCOO)_3]$, when compared to the Fe, Mn, Co, Zn, or Ni analogues, for which $T_c \approx 160-185$ K.[6] It has been argued that such a marked increase of the transition temperature in the magnesium compound could be attributed to more ionic metal−oxygen bonds in $[(CH_3)_2NH_2][Mg(HCOO)_3]$ and, consequently, stronger hydrogen bonds between the Mg-formate and the dimethylammonium (DMA) cations.[6] Our results show that $[NH_4][Mg(HCOO)_3]$ undergoes a ferroelectric phase transition at T_c = 255 K. This transition temperature is higher than that reported for M = Zn, Ni, Co, and Fe analogues ($T_c \approx 91-212$ K),[7,8] but practically the same as that reported for $[NH_4][Mn(HCOO)_3]$ (T_c = 254 K);[7] that is, T_c does not exhibit any significant increase when Mn^{2+} is replaced by Mg^{2+}. Thus, the model based on the more ionic metal−oxygen bonds in the magnesium analogues cannot explain the behavior of $[NH_4][Mg(HCOO)_3]$. Here it is important to mention than the dependence of the phase transition temperature on size of the M^{2+} ions was discussed by Xu et al. for other $[NH_4][M(HCOO)_3]$, with M = Fe, Mn, Co, Zn, or Ni.[7] It has been argued that the phase transition temperature decreases for smaller metal ions within the series because the framework becomes smaller, which means higher (internal) pressure for the 1D liquid−solid transition, together with lower freezing temperature.[7] This simple model also fails in the case of $[NH_4][Mg(HCOO)_3]$ since the ionic radius of Mg^{2+} (0.86 Å) is much smaller when compared with the ionic radius of Mn^{2+} (0.97 Å), but the both compounds undergo the phase transition at nearly the same temperature. Another possible scenario is that T_c increases for $[NH_4][Mg(HCOO)_3]$ due to a much smaller mass of Mg, which is only half less than that of Fe, Mn, Co, Zn or Ni, resulting in different lattice dynamics. However, this scenario also cannot explain very similar T_c values for the Mn- and Mg-compounds. We suppose, therefore, that T_c depends on both size and mass of the metal ions; that is, T_c increases with the decreasing mass and increasing size of the metal cations. T_c is also influenced by the type and size of the cation located in the large cavities, as evidenced by different effects of Mg^{2+} on T_c in the ammonium and dimethylammonium formates. Thus, the mechanism of the phase transition can be rationalized as follows. Upon cooling, the lattice shrinks, leading to a decrease of the framework space volume for accommodating NH_4^+. This in turn results in changes of the N···O bond distance as well as the N−H···O bond angle to maintain optimal hydrogen bonding between N−H and formate groups, leading to slowing down of the NH_4^+ movement and consequently to ordering of NH_4^+ at low temperatures.

dx.doi.org/10.1021/ic4020702 | Inorg. Chem. 2014, 53, 787−794

CONCLUSIONS

Our results indicate that $[NH_4][Mg(HCOO)_3]$ crystallizes in the $P6_322$ structure, in which the NH_4^+ cations are orientationally disordered. It exhibits a structural phase transition at approximately 255 K, associated with symmetry lowering to the ferroelectric $P6_3$ structure. It should be noted that the same structural changes previously have been reported for other $[NH_4][M(HCOO)_3]$ compounds with M = Mn, Co, Fe, Ni and Zn. However, in the previous report for other $[NH_4][M(HCOO)_3]$ compounds, the low-temperature structure was solved only at 110 K, that is, far below T_c,[7] whereas we present details of the low-temperature phase at three different temperatures, that is, at 248, 220, and 120 K. In this way, we have been able to show that not only the rotational but also translational dynamics of NH_4^+ plays a major role in the phase transition mechanism. In particular, crystallographic data reveal that translational dynamics of NH_4^+ located at three different sites in the LT phase is significantly different. Namely, translational motions of NH_4^+ shifted in the $(+c)$ direction freeze already just below T_c, whereas NH_4^+ shifted in the $(-c)$ direction exhibits gradual motional freezing with decreasing temperature. Our data also show that although in the LT ordered phase of $[NH_4][Mg(HCOO)_3]$ the three nitrogen atoms become inequivalent at the X-ray time scale, the rotational motion of NH_4^+ does not freeze completely at the phase transition but exhibits further slowing down below 255 K at the Raman and IR time scale. More precisely, Raman spectra show two features: (i) strong decrease in intensity of the N−H stretching bands with increasing temperature and (ii) strong increase in fwhm of the bands related to NH_4^+. These changes reflect the highly dynamic nature of the hydrogen bonds. Analysis of the temperature dependence of the fwhm shows that the dynamics of the NH_4^+ ions become important above 140 K.

Our results also indicate that the phase transition temperature increases with the decreasing mass and increasing size of the metal cations. The size of the cation located in the large cavities also has a significant impact on T_c. This result indicates a way to modulate the ferroelectric transition temperature and ferroelectric properties by changing the type of cation located in the large cavities and divalent cation in the metal formate framework.

ASSOCIATED CONTENT

Supporting Information

X-ray crystallographic information files (CIF) for crystal structures at 295, 248, 220, and 120 K. Figures S1−S8: Powder X-ray diffraction, imaginary part of the dielectric constant, distribution of NH_4^+ cations around trigonal axis in the crystal cages, IR and Raman spectra, temperature dependence of bandwidths and frequencies. Tables S1−S4: crystallographic data. This material is available free of charge via the Internet at http://pubs.acs.org.

AUTHOR INFORMATION

Corresponding Author

*E-mail: m.maczka@int.pan.wroc.pl; phone: +48-713954161; fax: +48-713441029.

Notes

The authors declare no competing financial interest.

ACKNOWLEDGMENTS

This research was supported by the National Center for Science (NCN) in Poland under project No. DEC-2011/03/B/ST5/01019.

REFERENCES

(1) (a) Rogez, G.; Viart, N.; Drillon, M. *Angew. Chem., Int. Ed.* **2010**, *49*, 1921−1923. (b) Ramesh, R. *Nature* **2009**, *461*, 1218−1219.
(2) (a) Wang, Z.; Zhang, B.; Otsuka, T.; Inoue, K.; Kobayashi, H.; Kurmoo, M. *Dalton Trans.* **2004**, 2209−2216. (b) Wang, X. Y.; Gan, L.; Zhang, S. W; Gao, S. *Inorg. Chem.* **2004**, *43*, 4615−4625.
(3) (a) Jain, P.; Dalal, N. S.; Toby, B. H.; Kroto, H. W; Cheetham, A. K. *J. Am. Chem. Soc.* **2008**, *130*, 10450−10451. (b) Jain, P.; Ramachandran, V.; Clark, R. J.; Zhou, H. D.; Toby, B. H.; Dalal, N. S.; Kroto, H. W; Cheetham, A. K. *J. Am. Chem. Soc.* **2009**, *131*, 13625−1327.
(4) Fu, D. W; Zhang, W.; Cai, H. L.; Zhang, Y.; Ge, J. Z.; Xiong, R. G.; Huang, S. D.; Nakamura, T. *Angew. Chem., Int. Ed.* **2011**, *50*, 11947−11951.
(5) Besara, T.; Jain, P.; Dalal, N. S.; Kuhns, P. L.; Reyes, A. P.; Kroto, H. W; Cheetham, A. K. J. *Proc. Nat. Acad. Soc. U. S. A.* **2011**, *108*, 6828−6832.
(6) Pato-Doldan, B.; Sanchez-Andujar, M.; Gomez-Aguirre, L. C.; Yanez-Vilar, S.; Lopez-Beceiro, J.; Gracia-Fernandez, C.; Haghighirad, A. A.; Ritter, F.; Castro-Garcia, S.; Senaris-Rodrigues, M. A. *Phys. Chem. Chem. Phys.* **2012**, *14*, 8498−8501.
(7) (a) Wang, Z.; Zhang, B.; Inoue, K.; Fujiwara, H.; Otsuka, T.; Kobayashi, H.; Kurmoo, M. *Inorg. Chem.* **2007**, *46*, 437−445. (b) Xu, G. C.; Zhang, W.; Ma, X. M.; Hen, Y. H.; Zhang, L.; Cai, H. L.; Wang, Z. M.; Xiong, R. G.; Gao, S. *J. Am. Chem. Soc.* **2011**, *133*, 14948−14951.
(8) Xu, G. C.; Ma, X. M.; Zhang, L.; Wang, Z. M.; Gao, S. *J. Am. Chem. Soc.* **2010**, *132*, 9588−9590.
(9) *CrysAlis RED, Data Reduction Program*, Issue 171.33.42; Agilent Technology: Poland.
(10) Sheldrick, G. M. *Acta Crystallogr. A* **2008**, *64*, 112−122.
(11) Guo, M.; Cai, H. L.; Xiong, R. G. *Inorg. Chem. Commun.* **2010**, *13*, 1590−1598.
(12) Li, W.; Probert, M. R.; Kosa, M.; Bennett, T. D.; Thirumurugan, A.; Burwood, R. P.; Parinello, M.; Howard, J. A. K.; Cheetham, A. K. *J. Am. Chem. Soc.* **2012**, *134*, 11940−11943.
(13) Shannon, R. D. *Acta Crystallogr. A* **1976**, *32*, 751−767.
(14) (a) Wang, C. H.; Wright, R. B. *J. Chem. Phys.* **1973**, *58*, 1411−1419. (b) Balusubramanian, M.; Ramakrishnan, V.; Rajendran, S. *Pramana - J. Phys.* **1991**, *36*, 603−610.
(15) (a) Maczka, M.; Hanuza, J.; Kaminskii, A. A. *J. Raman Spectrosc.* **2006**, *37*, 1257−1264. (b) Magalhaes, A. L.; Madail, S. R. R. S.; Ramos, M. J. *Theor. Chem. Acc.* **2000**, *105*, 68−76.
(16) Mookherjee, M.; Redfern, S. A. T.; Zhang, M.; Harlov, D. E. *Eur. J. Mineral.* **2002**, *14*, 1033−1039.
(17) Samantaray, R.; Clark, R. J.; Choi, E. S.; Dalal, N. S. *J. Am. Chem. Soc.* **2012**, *134*, 15953−15962.
(18) (a) Berger. *J. Phys. C* **1975**, *8*, 2903−2910. (b) Ayala, A. P.; Henriques Neto, J. M.; Paschoal, C. W. A.; Guedes, I.; Sasaki, J. M.; Freire, P. T. C.; Melo, F. E. A.; Medes Filho, J.; Leyva, A. G.; Polla, G.; Vega, D.; Perazzo, P. K. *J. Raman Spectrosc.* **2000**, *31*, 491−495. (c) Heyns, A. M. *J. Chem. Phys.* **1986**, *84*, 3610−3616.
(19) Maczka, M.; Waskowska, A.; Hanuza, J. *J. Solid State Chem.* **2006**, *179*, 103−110.
(20) Lautie, A.; Froment, F.; Novak, A. *Spectrosc. Lett.* **1976**, *9*, 289−299.
(21) (a) Smrcok, L.; Bitschnau, B.; Filinchuk, Y. *Cryst. Res. Technol.* **2009**, *44*, 978−984. (b) Kruger, A.; Heyns, A. M. *Vib. Spectrosc.* **1997**, *14*, 171−181.
(22) Popkov, Y. A.; Taranova, I. A.; Vankevich, A. V.; Savchenko, E. M. *J. Korean Phys. Soc.* **1998**, *32*, S613−S616.